Materials Advances

ROYAL SOCIETY OF CHEMISTRY

PAPER

View Article Online
View Journal | View Issue

Cite this: *Mater. Adv.*, 2025, **6**, 7016

Development and characterization of compressed unidirectional jute fibre-reinforced polylactic acid (PLA) composite materials

Rowshanuzzaman Kanon,[a] Ariful Islam,[a] Mainul Islam,[a] Emdadul Haq,[b] Hurazannat Monira[a] and Forkan Sarker *[a]

Received 26th May 2025,
Accepted 13th August 2025

DOI: 10.1039/d5ma00541h

rsc.li/materials-advances

Jute fibres have significant potential as a natural reinforcement in composite materials, particularly when these fibres are prepared and modified based on their grade and packing efficiency in dry fibre preforms. Highly packed unidirectional (UD) jute fibre preforms have been proven to possess excellent mechanical properties when combined with synthetic matrices, for example, epoxy, polyester, and polypropylene. However, very limited literature is available on the development of UD jute fibre-reinforced composites from biodegradable matrices such as polylactic acid (PLA). This work presents the development of highly compressed UD jute fibre preforms and composites from a PLA matrix. The results support the fact that compared to the mechanical properties of neat PLA, those of the composites improve significantly with an increase in the fibre content. At 50% fibre content, the composite achieved the highest tension strength of about ~187 MPa and flexural strength of approximately ~91.77 MPa. A comparative analysis shows that these composites can be viable alternatives to synthetic matrices such as epoxy, polyester, and polypropylene for many industrial applications.

1. Introduction

Natural fibre-reinforced composites play a critical role in many potential structural composite applications due to their higher specific properties compared to their synthetic counterparts. Jute is one of the most widely grown natural fibres, which can create an impact in meeting the demands of materials in many structural composite applications, such as the automotive, construction, and furniture industries.[1] Ideally, synthetic matrices such as polyester, epoxy, polypropylene, and polyethylene are commonly used with jute fibre reinforcement to ensure the higher load-bearing ability of composites.[2,3] However, these matrices are based on petroleum resources, which create major concerns for the end user as well as the manufacturer of the composites. Therefore, exploring sustainable and environmentally friendly materials for the fabrication of composites is in a great demand in the field of composite science and technology.[4,5] Alternatively, the development of composites using biodegradable and renewable matrices has emerged as a promising alternative to reduce environmental impact and dependence on fossil fuels.[6] Jute fibre-reinforced composites, when combined with biodegradable polymer matrices, offer dual benefits: they are lightweight and mechanically efficient, and they contribute to reduced greenhouse gas emissions and end-of-life waste management challenges.[7] This synergy of performance and sustainability positions them as ideal candidates for green material solutions. In recent years, growing environmental regulations and consumer demand for eco-friendly products have further accelerated the interest in using bio-composites.[8] Plant-based fibre composites have been widely explored by researchers for their mechanical performance across varying fibre loadings. It has been shown that increasing the fibre content in a composite tends to enhance both its tensile and flexural strength up to an optimal point, beyond which an excessive fibre loading can have detrimental effects on its strength and overall structural integrity.[9–11] For instance, composites made from kenaf fibre and PLA at 40 wt% fibre loading demonstrated flexural moduli in the range of 5 to 7 GPa and flexural strength values of 40 to 100 MPa.[12–14] When the fibre content was increased to 70%, the tensile strength of the kenaf sheet/PLA composites reached around 60 MPa. Bamboo fibres, known for their high modulus, are also considered potential replacements for synthetic fibres such as glass fibres due to their inherent strength, especially when aligned unidirectionally and used in long fibre formats. In contrast, coir fibres with low modulus and high strain characteristics have shown promise in delivering enhanced

[a] *Department of Textile Engineering, Dhaka University of Engineering & Technology, Gazipur, Bangladesh. E-mail: forkan@duet.ac.bd*
[b] *Department of Textile Engineering, National Institute of Textile Engineering and Research (NITER), Bangladesh*

elongation and impact resistance in PLA composites, making them suitable for structural applications in buildings, as well as for sound and thermal insulation purposes.[10,15–17]

Natural fibre composites, particularly those reinforced with jute, offer several mechanical advantages, including high specific strength, moderate stiffness, low density, and good damping properties, making them suitable for semi-structural and structural applications.[18,19] Current jute fibres as a reinforcement in composites have different common architectures, including loom-based woven structures, which are formed by the interlacement of two yarns, knitted structures formed by the interloping of two vertical and horizontal yarns, and braided structures. A range of derivatives from these three principal manufacturing techniques is commonly featured as dry fibre preforms in composite fabrication in both thermoplastic and thermoset composite applications.[20–22] However, the manufacturing of these textile architecture preforms requires a long timeframe with a lot of work force, which leads to an increase in the cost of reinforcement in composites. Besides these drawbacks, either interlacement or interloping of yarns creates a lot of micro voids or porous structures to generate crimps, which ultimately significantly impact the development of stress in composites. Moreover, the twist in the yarns creates impregnation problems during consolidation, which ultimately results in more voids in the composites. Therefore, the use of these structures results in a drastic reduction in the mechanical properties of composites. Scientists recently identified these drawbacks and extensively studied how to enhance the mechanical properties of natural fibre-reinforced composites. It is influenced by the study of the rule of mixture that placing the fibres in the parallel direction can only ensure one hundred percent utilization of the fibre load-bearing ability in composites. However, placing jute fibres in the parallel direction is troublesome due to the presence of helical interfibrillar networks in these technical fibres. Thus, to address these issues, Sarker *et al.* found that using field-retted fibres and their subsequent physical and mechanical modification can ensure the greater utilization of the fibres in the parallel direction.[23] Their study recommended that highly cleaned raw jute fibres can be individualized to single fibres without physical damage to the fibres, and this can enhance the single-fibre strength to more than ~30–40%. Moreover, light compression of these individualized fibres with mist can significantly enhance their packing compared to the unmodified dry fibre preforms. However, the role of fibre content in the preforms and composites in the literature has not yet been explored completely with the selective matrices commonly used in the fabrication of composites. This means that the mechanical properties of the composites can be increased with an increase in the packing of fibre and the maximum alignment of the fibres in the parallel direction ensured. Hence, achieving a higher fibre packing along with fibre alignment in the composite structure can significantly improve its mechanical performance by reducing internal voids and maximizing stress transfer.[24]

When considering the selection of bio-composite matrices, their compatibility with the environment is crucial. The common biodegradable or compatible matrices include polylactic acid (PLA), polyhydroxybutyrate (PHB), polybutylene succinate (PBS), polycaprolactone (PCL), starch-based polymers, and cellulose-based polymers.[25–27] However, their uses are mainly limited to medical and biomedical applications, agriculture, 3D printing, disposable items, and recently, in flexible composites. The main reason for using these matrices is their degradability when used with natural fibres, reduction of carbon footprint, and reduction of the reliance on petroleum-based polymers.[28–30] Among them, PLA has attracted considerable interest due to its availability, processability, and mechanical characteristics, which are moderately suitable for various applications.[31,32] In the development of fully biodegradable composites using jute fibres, most of the work is related to using PLA with short fibres, while mixing it with fibres in twin screw extrusion to manufacture modified pellets and further with compression moulding to manufacture composites. However, this way of manufacturing composites results in very low mechanical properties. The highest properties shown by short fibre-based jute/PLA composites were strength of ~79 MPa and stiffness of ~5 GPa only.[33] At the same time, using traditional fabric, the strength of the composites was reduced to ~45 MPa and the stiffness of the composites to 16.5 GPa.[33] Alternatively, when other fibres, such as kenaf and coir fibres, were hybridized with a PLA matrix, the composites achieved the higher tensile strength of ~100 MPa and the stiffness of ~7 GPa.[34] These studies reported that PLA shows relatively lower strength, and the fiber architecture limitation lowers the overall performance of the composites. Other fibres, such as flax, have been used in unidirectional arrangements, and when mixed with PLA matrices, the maximum tensile strength and stiffness of the composites were found to be ~339 MPa and ~21 GPa, respectively.[35] Despite the promising results of other natural fibres in UD form, research on unidirectional (UD) jute fibre-reinforced PLA composites remains extremely limited. However, the application of UD jute fibres with a PLA matrix is limited in the literature. Therefore, this study was strongly influenced by determining the role of UD jute fibres with PLA matrices in the development of biodegradable composites.

To the best of our knowledge, the potential of highly packed UD jute fibre preforms and PLA matrix-based composites has never been explored in the literature. In this study, a highly viscous PLA matrix was applied to acquire UD jute fibres and the impact of the content of jute fibres in composites noted through compression moulding techniques. The mechanical properties of the composites were evaluated based on the role of the fibres in the composites. This research focuses on utilizing highly aligned jute fibres in unidirectional (UD) preforms to optimize the mechanical performance and increase the fibre volume fraction in the resulting composites. The goal is to improve both the tensile and flexural characteristics of the jute-reinforced PLA composites. Key investigations included the assessment of tensile strength, flexural behavior, water absorption capacity, and fibre–matrix interfacial bonding, where the latter was examined through scanning electron microscopy (SEM). Some numerical simulations were employed to validate the experimental findings and identify potential

variations in the properties linked to the new UD jute/PLA composite. Additionally, the practical implications of this study extend to the design of biodegradable and high-strength composites for use in Metrorail interiors, automotive interiors, lightweight construction materials, packaging solutions, eco-friendly furniture components, agricultural equipment panels, and sustainable consumer products. A comparative analysis was also conducted to evaluate how the developed composite performs relative to other recently used natural fibres in the fabrication of composites.

2. Methodology

2.1 Materials

Field-retted jute fibres (*Corchorus olitorius*), also locally known as Tossa Jute, were collected from the east river coastal area of Bangladesh, where farmers have their primary choice of cultivating these fibres due to their large demand in the local spinning industry. Table 1 contains the physical and mechanical properties of the jute fibre. Polylactic acid (PLA) is an eco-friendly, biodegradable thermoplastic polymer pellet that has been purchased from Modern Scientific Co. Ltd, Hatkhola, Bangladesh. The melting point of PLA ranged from 160 °C to 170 °C. The specifications of the properties of PLA can also be seen in Table 1.

2.2 Methods

2.2.1 Jute fibre preform development. The development of jute fibre preforms involves several important steps to transform raw jute fibres into a structured material for the fabrication of composites (see Fig. 1a). It begins with cleaning the fibres to remove impurities such as shives, dust, and contaminants using mechanical and manual techniques. The cleaned fibres are sun-dried to reduce moisture, preserving their strength and integrity. This is followed by preconditioning to ensure a uniform moisture content and flexibility. Hackling then aligns the fibres and removes the short fibres and remaining impurities, enhancing the mechanical properties by making the fibres parallel, as shown in Fig. 1b and c.

1% of starch is applied to bind the fibres (see Fig. 1d), ensuring they maintain their shape and structural integrity

Table 1 Measured properties of the composite constituents used in this study

Composite constituent	Density, g cm^{-3}	Diameter, mm	Strength, MPa	Stiffness, GPa	Fibre length, mm	Fibre aspect ratio, mm	Fibre critical length, mm	Length efficiency for stiffness	Length efficiency for strength
Jute fibre	1.48	0.05	280	24	122	2422	2.82	0.998	0.989
PLA resin[a]	1.25	—	25	2.2	—	—	—	—	—

[a] Indicates value collected from the previous study.[35]

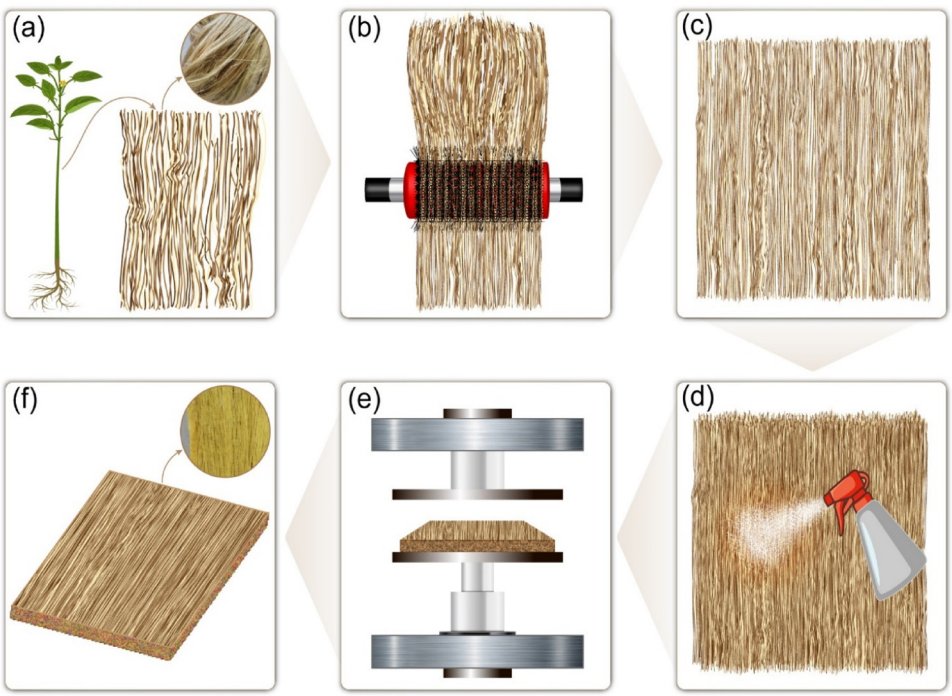

Fig. 1 Schematic of preform (UD) preparation: (a) raw long jute from jute plants, (b) fibre hackling process, (c) aligning long jute, (d) applying 1% starch, (e) compression moulding, and (f) jute fibre preform.

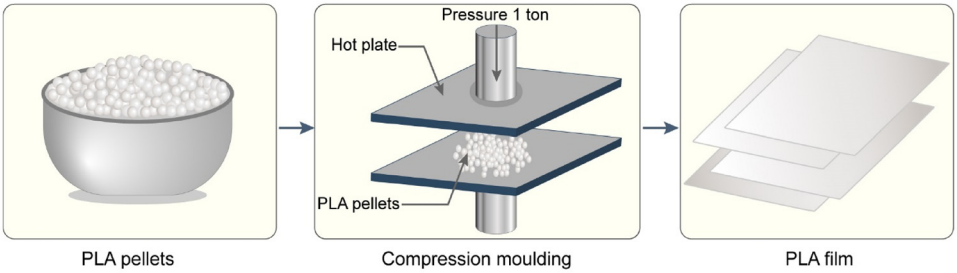

Fig. 2 Preparation of PLA film from PLA pellets by compression molding machine.

during handling and moulding. Starch is chosen for its excellent adhesive properties and compatibility with jute fibres.

After applying the binder, the jute fibre preform undergoes compression moulding, where heat and pressure consolidate the fibres into a solid, cohesive structure, as shown in Fig. 1e. This enhances the bonding between the fibres and the binder, resulting in a strong, durable material. 3 tons pressure and temperature of 110 °C are applied and maintained for 5 min. The final step involves cutting and shaping the preform to the desired dimensions. Key physical properties, including basis weight (200–400 gsm), thickness (0.3 cm), and dimensions (20 cm × 15 cm × 0.3 cm), are measured to ensure quality. The development of jute fibre preforms combines traditional and modern techniques to create a sustainable, high-performing material (see Fig. 1f). Jute fibres are biodegradable and sourced from renewable resources, meeting the demand for eco-friendly materials. The systematic process of cleaning, drying, preconditioning, hackling, binding, and compression moulding produces high-quality jute fibre preforms for various applications, ranging from automotive components to construction materials.

2.2.2 Preparation of PLA films. PLA (polylactic acid) films were fabricated first as matrix materials before the production of green jute/PLA biocomposites. The compression-moulding process at 170 °C allowed PLA granule melting and generated smooth thin films through 1 ton per square inch (psi) of constant pressure application. Manufacturing equipment formed the molten PLA into thin, uniform films with a thickness of approximately 1.5 mm. These films were then cooled and cut into standard dimensions of 300 mm × 300 mm, aligning with the mould size used in composite fabrication, as demonstrated in Fig. 2. Qualitative assessment systems verified that the films underwent strict quality control, which eliminated bubbles, voids, and contamination. The films were carefully handled and stored to maintain their structural integrity until the stage of fabrication.

2.2.3 Preparation of jute/PLA green biocomposites. The manufacture of green jute/PLA biocomposites followed a controlled procedure to produce a high-quality and environmentally friendly material. The process began with preparing a clean and contaminant-free mould, with dimensions of 300 mm × 300 mm, to which a demoulding agent was applied for easy removal of the finished composite. A Teflon sheet was

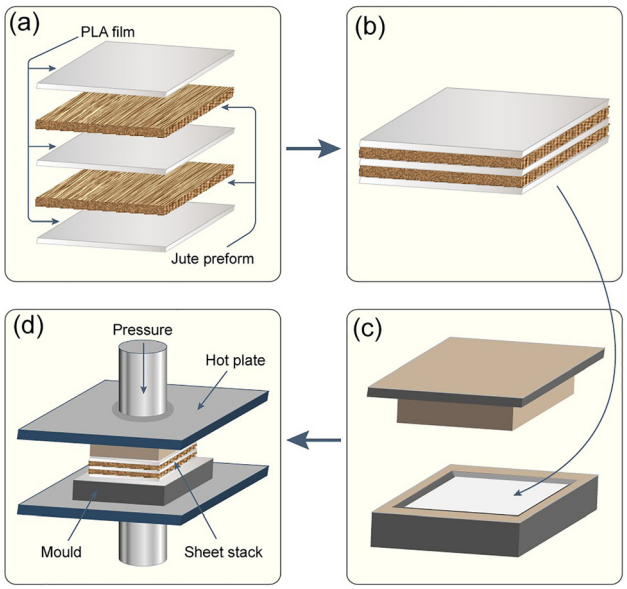

Fig. 3 Schematic of the jute/PLA UD composite fabrication process: (a) stacking sequence of composites, (b) jute/PLA sheet stack, (c) moulding mould, and (d) composite fabrication.

placed inside the mould as an anti-adhesion film to obtain a good, smooth surface finish and keep it from sticking to the mould. Jute fibre preform and PLA film stacks (with matching dimensions of the mould) were aligned in the mould, as shown in Fig. 3a–c. Moulding was performed at a temperature of about 170 °C, which melted PLA and effectively impregnated the jute fibres, and pressure of up to 3 tons per square inch (psi) was used to help the melted PLA flow around the fibres for uniform distribution with strong binding. The pressure was held for 15 min, thus making sure the fibres were completely encapsulated, as demonstrated in Fig. 3d. Maintaining the right temperature and pressure for the appropriate duration is crucial to achieving the optimal mechanical properties and integrity of biocomposites.

After the required time, the mould is gradually cooled, solidifying the PLA matrix and locking the jute fibres in place. Once cooled, the composite is removed from the mould with the help of the demoulding agent and Teflon sheet, ensuring it retains its shape and surface quality. The final step involves trimming the biocomposites to the desired dimensions and

inspecting their properties such as thickness, density, and surface quality to ensure that they meet standards. These properties are also crucial for their performance in applications such as automotive, construction, and consumer goods, making it essential to modulate the surface energy at the nanoscale for wettability control. Bio-composites based on jute and PLA are eco-friendly substitutes for conventional materials owing to their strength, stiffness, and other environmental advantages. The fabrication process, including mould preparation, the application of demoulding agents, placement of Teflon sheet, temperature and pressure parameters and controlled cooling, results in a very good end product.

2.3 Characterization of composite

2.3.1 Tensile strength. A universal testing machine (UTM) from Shimadzu AGS-X, Japan was used to conduct the tensile test. The ASTM D-638 standards were followed to break the sample under a pressure of 20 kN. During the testing phase, 5 mm min^{-1} was the speed of the crosshead of the machine, and the gauge length was fixed at 50 mm. The above-mentioned standard was followed in the preparation of the 165 mm length and 15 mm width tensile test specimens. After examining each of the three sample types, the average collected data was used to determine the final results.

2.3.2 Flexural testing. Following the ASTM D-790 standards, a three-point bending test was performed using a universal testing machine (UTM). Each specimen had dimensions of 125 mm in length and 12.4 mm in width, with the support span set at 50 mm. For each sample category, at least three specimens were tested under a crosshead speed of 1.4 mm min^{-1}.

2.3.3 Thermogravimetric analysis (TGA). The thermal stability of the unidirectional jute fibre-reinforced PLA green composites was evaluated using thermogravimetric analysis (TGA). Approximately 25 mg of each sample was gradually heated in a nitrogen atmosphere using an SDT650 thermal analyzer. The temperature range for the analysis extended from 30 °C to 500 °C, at a controlled heating rate of 10 °C per minute.

2.3.4 Water absorption. ASTM D 570-99 was followed for the evaluation of the water uptake (wt%) by the composites. The size of the test specimen dimensions was 39 mm × 10 mm. The sample pieces that had been sliced were placed in an oven set to 105 °C for a minimum of one hour to eliminate any surplus moisture. Following that, the samples were collected to weigh them in a precision balance designated as W_1. Then 48-h immersion in water was applied to the composite sample. Following another weighing, the damp sample was cleaned with tissue paper. After the sample was submerged in water, its weight was W_2. Next, the following formula was used to determine the water uptake amount:

$$W_A(\%) = \frac{W_1 - W_0}{W_0} \times 100\% \quad (1)$$

where W_A stands for water absorption, W_1 for the weight of the composite following water immersion, and W_0 for the weight of the composite before water immersion.[36]

2.4 Theoretical modelling

2.4.1 Density and porosity measurement of composites. This work assessed the composite densities using an AJ5OL analytical balance (Mettler, Toledo, UK) ASTM-D3800-99 approach. The literature[37] provides thorough details about this test. Briefly, both in air and in water, jute and banana mono and hybrid composites were weighed. The buoyant force is shown by the weight difference between the water and air readings. Then the density of the composite was computed with reference to the following eqn (2). Eqn (3) helped to determine the theoretical density of the composites.

$$\rho_C = \frac{M_1}{(M_1 - M_2)}(\rho_w - \rho_a) + \rho_a \quad (2)$$

where ρ_C is the density of the composites, M_1 and M_2 are the weights of sample in air and in water, respectively, ρ_w is the density of water, which is 0.9982 g cm^{-3}, and ρ_a is the density of air, which is 0.0012 g cm^{-3}.

$$\rho_{thc} = \frac{1}{\frac{W_f}{\rho_f} + \frac{W_m}{\rho_m}} \quad (3)$$

where ρ_{thc} is the theoretical density of the composites, W_f and W_m are the weights of the fibre and matrix, and ρ_f and ρ_m are the density of jute fibre PLA matrix, respectively.

2.4.2 Rule of mixture (RoM). Eqn (4) can be used to determine the relationship between the volume fraction and weight fraction of the composite constituents in the rule of mixture system. The density of the composites in a singular system can be determined using eqn (2) and (3), as outlined in the preceding section.

$$V_f = \frac{\frac{W_f}{\rho_f}}{\frac{W_f}{\rho_f} + \frac{W_w}{\rho_m}} \quad (4)$$

where V_f is the fibre volume fraction in the composites. W_f and W_m are the weight fraction of the fibre and matrix in the single system of composites, respectively, ρ_f = fibre density and ρ_m = matrix density. In the case of individual fibres in the hybrid composite system, the fibre volume fraction of each fibre can be determined using eqn (4).

Given that all the fibres in the composites are organized in the parallel direction, the RoM formula can be used to forecast their tensile characteristics (modulus and strength). Furthermore, the connection between the matrix and fibre is excellent, with the absence of voids inside the composites. The applied loads also follow either the parallel or normal direction of the fibre.[38] Eqn (5) and (6) can be used to anticipate the tensile strength and modulus of the composites, respectively.

$$E_c = E_f V_f + E_m V_m \quad (5)$$

$$\sigma_c = \sigma_f V_f + \sigma_m V_m \quad (6)$$

where E_c, E_f and E_m are the modulus of composite, fibre and matrix, and σ_c, σ_f and σ_m are the strength of the composites, fibre, and matrix used in the study, respectively.

2.4.3 Halpin-Tsai model. The semi-empirical Halpin-Tsai model, as expressed in eqn (7) and (8), was employed to estimate the tensile strength and Young's modulus of the discontinuous fibre-reinforced composites aligned in both the longitudinal and transverse orientations.

$$\sigma_c = \sigma_m\left(\frac{1+\zeta\eta V_f}{1-\eta V_f}\right) \tag{7}$$

$$E_c = E_m\left(\frac{1+\zeta\eta^* V_f}{1-\eta^* V_f}\right) \tag{8}$$

where η and η^* are given by:

$$\eta = \frac{\frac{\sigma_f}{\sigma_m}-1}{\frac{\sigma_f}{\sigma_m}+\zeta} \tag{9}$$

$$\eta^* = \frac{\frac{E_f}{E_m}-1}{\frac{E_f}{E_m}+\zeta} \tag{10}$$

Also, the shape fitting parameter ζ in the Halpin-Tsai model is used to correlate theoretical predictions with experimental data and is dependent on the fibre geometry as well as the loading direction, either longitudinal or transverse to the fibre orientation. In the case of fibres with a circular cross-section, ζ is typically defined as follows:

$$\zeta = \frac{2l}{d} \tag{11}$$

where l is the length of the fibre in the load direction, and d is the fibre diameter (so that ζ can be assumed to be 2 for transverse tensile properties).[39]

2.4.4 Kelly and Tyson's equation. The mechanical behaviour of fibre-reinforced composites is significantly influenced by parameters such as critical fibre length (l_c), initial fibre length (l_f), fibre diameter (d_f), and aspect ratio $\left(\frac{l_f}{d_f}\right)$. In these studies, natural fibres with relatively high critical fibre lengths, ranging from 0.9 to 2 mm, have been utilised.[40–42] Eqn (13) helped to find the length efficiency factor. Eqn (13) was employed to find the length efficiency factor, while eqn (14) and (15) were used to estimate the tensile modulus and tensile strength of the composites, respectively.

$$l_c = \left(\frac{\sigma_f x D}{2x\tau}\right) \tag{12}$$

$$\eta_{iS} = 1 - \frac{l_c}{2l_f} \text{ for } l_f \geq l_c \tag{13}$$

$$\sigma'_m = E_m\varepsilon_c \tag{14}$$

$$\sigma_c = \eta_0\eta_{iS}\sigma_f V_f + \sigma'_m V_m \tag{15}$$

To calculate the length efficiency factor for stiffness, the (η_{IE}) Cox shear lag model was applied.[43] The application of eqn (16) assists in determining the axial loading of fibres, and the elastic strain transfer adopts the iso-strain characteristic between the fibre and matrix.

Where G_m is the shear modulus of the matrix, which is determined based on the information given by the supplier, while the fibre stiffness E_f is experimentally measured. Also, parameter k accounts for the maximum packing efficiency or volume fraction of fibres within the composite.

$$\eta_{IE} = 1 - \frac{\tanh\left(\frac{\beta l_f}{2}\right)}{\frac{\beta l_f}{2}} \tag{16}$$

$$\frac{\beta l_f}{2} = 2x\frac{l_f}{D}X\sqrt{\frac{G_m}{E_f \ln\left(\frac{k}{V_f}\right)}} \tag{17}$$

$$G = \frac{E_m}{2(1+\vartheta_m)} \tag{18}$$

$$E_c = (\eta_0\eta_{IE}E_f V_f + E_m V_m) \tag{19}$$

The different variables related to the fiber and resin were obtained from the calculated values in Table 1.

3. Results and discussion

3.1 Tensile properties

Fig. 4b presents the typical stress–strain plots of the F20P80 and F50P50 composites for comparative analysis. It can be observed that both composites have brittle behaviour with significant yielding as their fibre content increases. Additionally, it is worth noting that the failure strain of all the composites is more than 4%, and this can be explained due to the high toughness of the biodegradable PLA matrix. These results are consistent with previous investigations on other natural fibre-based composites based on a PLA matrix.[44,45] In this study, non-linearity was observed in the stress–strain curves of the composites. A couple of important factors can be considered for this type of behaviour.

Natural fibres always exhibit a viscoelastic trend in their stress–strain curves due to their inherent binding materials, such as hemicelluloses, lignin, and waxes. Therefore, the performance of composites is affected in a similar manner. In addition, single fibres within composites break first, and then the load is transferred to the fibre network, which affects the linearity in the stress–strain curve of the composites.[1]

This study investigates the influence of unidirectional (UD) jute fibre content on the tensile performance of PLA-based composites, as illustrated in Fig. 4a. Fibre loadings ranging from 20% to 50% by volume were selected, given that the

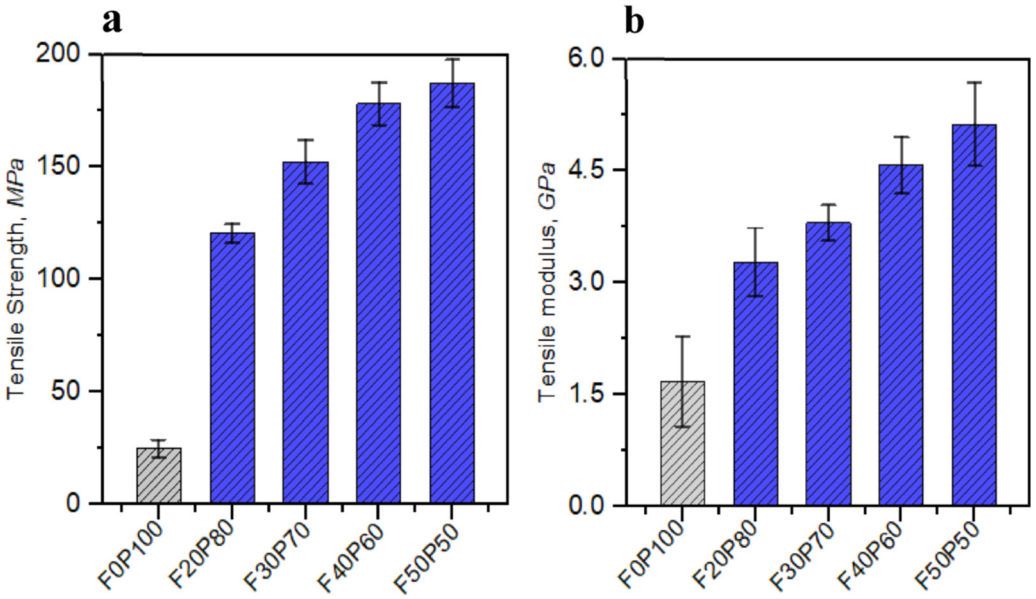

Fig. 4 Tensile properties of UD jute-PLA biocomposites with respect to fibre weight fraction: (a) tensile strength of composites and (b) tensile modulus of composites.

composites containing less than 20% exhibited significantly reduced tensile properties, while fibre contents exceeding 50% may lead to a degradation in performance due to the formation of fibre networks.[46] The experimental results demonstrate that incorporating UD jute fibres substantially enhances both the tensile strength and modulus compared to neat PLA. For instance, the F20P80 composite, containing 20% jute fibre, achieved a tensile strength of approximately 120 MPa and a tensile modulus of around 3.28 GPa, representing improvements of about 380% and 95%, respectively, over the pure PLA matrix. These enhancements are attributed to the alignment of the jute fibres along the tensile axis, effective separation of the field-retted fibres, and robust interfacial bonding between the fibre and matrix. Furthermore, the F50P50 composite with 50% fibre content attained a maximum tensile strength of roughly 187 MPa and a tensile modulus of approximately 5.1 GPa. This considerable improvement is likely due to the more uniform fibre packing during the preforming stage, where the individual fibres form a well-aligned structure, fostering stronger interfacial adhesion between the fibres and the PLA matrix.

3.1.1 Comparison of experimental and numerical model results. Fig. 4a illustrates a comparative analysis between the experimentally obtained tensile strength values and that predicted by various established theoretical models, while Fig. 4b depicts the corresponding tensile modulus data. The models considered include the rule of mixtures, Halpin-Tsai model, Kelly-Tyson model, and Cox shear-lag theory. These numerical predictions based on the intrinsic properties of the matrix and reinforcing fibres (as detailed in Tables 2 and 3) offer an estimation of the mechanical behavior of composites. The experimental findings serve as a reference point for validating the predictive accuracy of these models. Each theoretical approach is based on distinct assumptions regarding fibre orientation, fibre–matrix interfacial bonding, and the influence of structural imperfections within the composite system.

Table 2 Comparison of tensile strength of the composites with numerical model data

Sample code	Experiment	RoM	Halpin-Tsai	Kelly	Cox
F20P80	120.74	71.775	72.09421	130.1604	128.7287
F30P70	152.43	100.79	97.82057	164.5585	162.7484
F40P60	178.32	123.58	119.7348	193.0929	190.9689
F50P50	187.37	153.631	148.6431	223.4847	221.0263

Table 3 Comparison of tensile modulus of composites with numerical model data

Sample code	Experiment	RoM	Halpin-Tsai	Kelly	Cox
F20P80	3.28	5.658	5.799995	5.336617	5.377313
F30P70	3.81	8.06352	8.0531	7.430806	7.495272
F40P60	4.58	9.98304	9.971439	9.213978	9.299268
F50P50	5.13	12.51413	12.50235	11.56528	11.67885

The rule of mixtures (RoM) provides a straightforward prediction based on a linear combination of the fibre and matrix strengths. In this model, it was found that composites with a lower fibre content (20%) show a significant disparity in tensile strength, being nearly 69.5% lower than the experimental tensile strength. However, the difference between the two results decreases as the fibre content in the composites increases. Specifically, at 50% fibre content, the disparity between the composite tensile strength and the RoM model reduces to approximately 21.97%. The disparity between the experimental tensile strength of the composites and the predictions from the rule of mixtures (RoM), particularly at lower fibre content (20%), can be attributed to several factors. The ROM assumes

ideal load sharing between the fibres and the matrix, with perfect fibre–matrix adhesion, which often does not reflect the actual behavior of fibre-reinforced composites. At a low fibre content, the matrix phase, being weaker, dominates the mechanical performance, leading to poor load transfer and a 69.5% lower tensile strength compared to the experimental results. Additionally, the RoM does not account for fibre distribution issues, which are more prevalent in low-fibre composites. Uneven fibre distribution, clustering, and matrix-rich regions create localized stress concentrations and further reduce the load-bearing efficiency. As the fibre content increases (*e.g.*, 50%), the disparity between the RoM and experimental values reduces (to 21.97%) because the fibres form a more interconnected network, which improves the load transfer and better supports the applied stress. At higher fibre contents, imperfections such as fibre misalignment have a smaller impact due to the increased fibre dominance. This leads to a closer alignment between the RoM predictions and experimental results, given that the behaviour of the composite approaches the idealized assumptions of the RoM. Hence, the RoM performs better at higher fibre contents, but it significantly overestimates the tensile strength when the fibre content is low. In the previous study by Efendy and Pickering, they observed a 21% difference in the predicted and experimental tensile strength of harakeke/PLA biocomposites.[47] This large difference with respect to the fibre content of natural fibre composites has been reported in another previous study.[48]

In the case of the Halpin-Tsai model, it can be seen that a lower fibre content shows large differences in the composite properties, and it follows a similar trend as the RoM model, where with an increase in the fibre content in the composites, the difference between the properties is reduced. Thus, it signifies the importance of fibre geometry in determining the composite mechanical properties. For better explanation, in this model, a perfect fibre–matrix interface and uniform stress distribution have been considered, but natural fibres such as jute are completely variable fibres, which come with a lot of impurities that impact the aspect ratio of the fibres. This may lead to a complex phenomenon between the fibres and matrix that has a chance of creating strong mechanical interlocking to ensure proper stress development in the composites. However, in this model, this significant improvement in stress transfer from the fibre to the matrix is not considered. This may be responsible for the big different in the experimental and model-based tensile strength of the jute fibre composites. This agreement is supported by the study of Nazrima *et al.*[49] with jute-polypropylene biocomposites from field-retted jute fibre.

The Kelly-Tyson model showed perfect alignment with the experimental results considering various fibre contents in the composites. At a 20% fibre content, the discrepancy between experiment tensile strength and model tensile strength of the composites is found to be 7.75%, and in the case of 50% fibre content, the difference is 19.22%, which is considerable for aligned natural fibre composites. The good alignment between the Kelly-Tyson model and the experimental tensile strength results for natural fibre composites can be attributed to several key factors. The Kelly-Tyson model accurately accounts for fibre length and aspect ratio, which are crucial in determining the load transfer efficiency in short-fibre composites such as those reinforced with natural fibres. This is particularly important because natural fibres often have high aspect ratios, which enhances their ability to carry loads effectively. This model considers imperfect fibre–matrix bonding, which is realistic for natural fibres that exhibit mechanical interlocking due to their rough surfaces. This improves the load transfer, especially at lower fibre contents, resulting in smaller discrepancies between the predicted and experimental tensile strength such as the 7.75% difference at a 20% fibre content. The Kelly-Tyson model is well-suited for unidirectional composites, where fibre alignment in the load direction maximizes the strength closely matching experimental results. Its effectiveness at predicting the tensile strength of both short and moderately long fibres further explains the good agreement with the experimental data. The sensitivity of this model to the fibre volume fraction accurately reflects the performance at different fibre contents with a 19.22% discrepancy at 50% fibre content due to the increased fibre contribution to the overall strength. Owing to these combined factors, the Kelly-Tyson model is highly effective for predicting the tensile strength of natural fibre composites.

The Cox model provides a good fit for the experimental tensile strength of natural fibre composites with a difference below 10% due to its consideration of the ''shear lag effect,'' which accurately captures how load is transferred from the matrix to the fibres. This model accounts for imperfect load transfer along the fibre length, which is particularly relevant in natural fibre composites where fibre–matrix bonding may not be ideal. The Cox model considers the fibre length and aspect ratio, which are essential factors for accurately predicting the tensile strength of composites, and also supports other works on natural fibre composites in the literature.[50] Its ability to model a partial fibre loading when not all fibres carry the load equally further improves its accuracy. The inclusion of these realistic factors allows the Cox model to provide more precise predictions for natural fibre composites, resulting in a good agreement with the experimental results.

While comparing the Young's modulus of the composites with the predicted models, it was found that almost all the models underestimate the Young's modulus of the composites, which can be seen in Table 3. At a lower fibre content (20%) and higher fibre content (50%), only the Cox model showed closer values than the other models reported in this study. Cox model predictions of the Young's modulus of jute fibre-reinforced composites are commonly reported in the literature, likely due to its consideration of specific fibre characteristics (such as fibre radius) and matrix properties (such as shear modulus). Although the predicted values across different models show relatively minor variations, notable discrepancies remain. Based on the Cox model, the deviation in Young's modulus at a 20% fibre content was calculated to be 63.71%, increasing to 127.49% at a 50% fibre content. In comparison, previous studies have reported discrepancies as high as 300% for the Young's modulus of natural fibre composites.[51,52]

The increasing discrepancy between the experimental Young's modulus and the Cox model predictions, particularly from 63.71% at a 20% fibre content to 127.49% at a 50% fibre content, can be attributed to several factors related to the limitations of the Cox model and the behaviour of the fibre-reinforced composites. One of the primary issues is the shear lag effect, which diminishes in efficiency as the fibre content increases. The Cox model assumes effective load transfer from the matrix to the fibres through shear, but at a higher fibre content, the fibres are more closely packed, leading to a decrease in the load transfer efficiency.[53] This phenomenon explains the smaller discrepancy at a 20% fibre content, where the fibres are better dispersed, but a much larger discrepancy at 50%, where fibre crowding hinders stress transfer. Additionally, the fibre–matrix interaction plays a crucial role. At higher fibre contents, the ability of the matrix to efficiently bond with and transfer stress to the fibres becomes limited. Natural fibres often have imperfect fibre–matrix adhesion, leading to weaker load transfer, especially at a higher fibre content.[54] This causes the Cox model, which assumes ideal bonding, to overestimate the Young's modulus as the fibre content increases. Another contributing factor is the nonlinear behavior of fibres at higher contents. Although the Cox model assumes a linear relationship between the fibre volume fraction and composite modulus, this is not the case in reality. Fibre misalignment, clustering and void formation become more pronounced as the fibre content increases, leading to a larger deviation from model predictions.[50] At a lower fibre content (20%), these issues are less prevalent, resulting in better agreement with the experimental results. Finally, the fibre packing and distribution at higher fibre contents create defects such as voids and fibre–fibre interactions that the Cox model does not account for. Given that the fibres are packed closer together at a 50% content, the presence of these defects reduces the overall stiffness of the composite, increasing the discrepancy between the experimental and predicted values.

3.2 Flexural properties

As illustrated in Fig. 5, the flexural behavior of jute-PLA biocomposites, specifically their flexural strength and modulus, offers meaningful insights into their mechanical performance and suitability for structural applications. This section evaluates both parameters to provide a holistic view of how varying the fibre content influences the performance of the composite. An increase in fibre loading from 20% to 40% leads to a notable enhancement in both the flexural strength and stiffness. The flexural strength increased from 82 MPa for the F20P80 composite to 91 MPa for the F40P60 variant, while the flexural modulus increased from 3.83 GPa to 6.61 GPa across the same range. These improvements indicate that incorporating jute fibres up to 40% by volume significantly reinforces the ability of the composite to withstand bending forces and contributes to greater material rigidity. The maximum flexural properties of strength of 91 MPa and modulus of 6.61 GPa for are observed at the 40% fibre content, as presented in Fig. 5. At this optimal fibre content, the composite achieves the best balance of load-bearing capacity and stiffness. The fibres effectively reinforce the PLA matrix, enhancing the overall mechanical performance. This optimal point likely represents the best synergy between the fibres and the matrix, where the stress transfer and dispersion are the most efficient.

At a fibre content of 50%, the F50P50 composites exhibit a flexural strength of 62 MPa and a flexural modulus of 5.97 GPa, indicating a noticeable reduction in both properties. This decrease can be explained by several underlying factors, as follows: (a) a weakened fibre–matrix adhesion, where an excessive fibre loading may compromise the interfacial bonding, limiting the effective stress transfer; (b) a poor fibre dispersion,

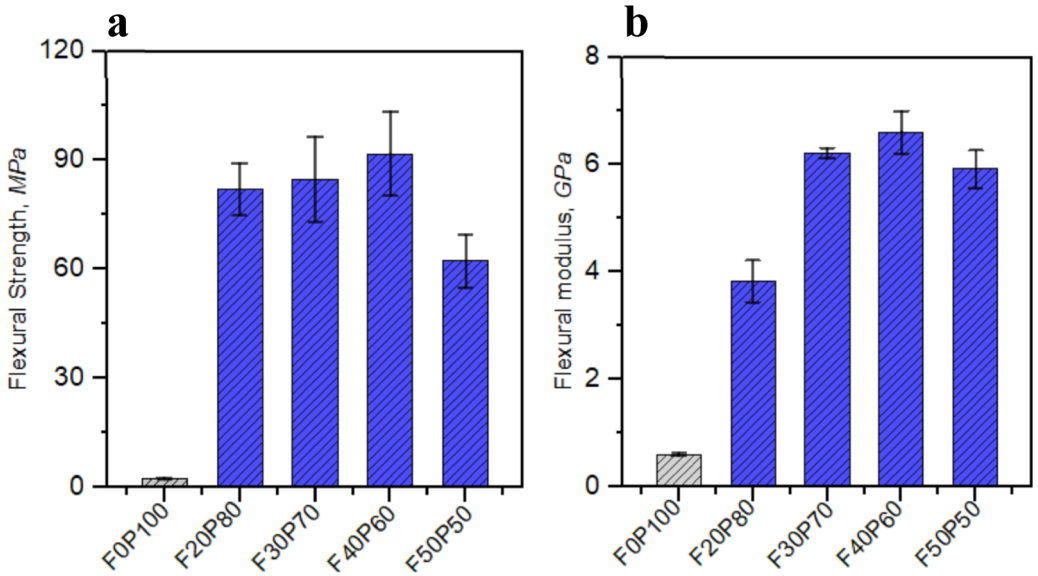

Fig. 5 Flexural properties of UD jute-PLA biocomposites with respect to fibre weight fraction: (a) flexural strength of composites and (b) flexural modulus of composites.

where higher concentrations of fibre can result in agglomeration, which acts as stress concentrators and promotes premature failure; and (c) matrix deficiency, where a lower proportion of matrix material may be inadequate to fully embed and bond the fibres, ultimately impairing the structural integrity of the composite.

3.3 Water uptake

Water absorption is a critical parameter for biocomposites, especially for those intended for use in environments where moisture exposure is inevitable. The water absorption characteristics of composites can significantly affect their mechanical properties and long-term performance. The water absorption properties of the jute-PLA-based bio-composites with varying fibre contents (20%, 30%, 40%, and 50%) were investigated to understand how fibre content influences the behaviour of the composite under wet conditions. The results indicated that water absorption increases with the fibre content in the biocomposites. The F20P80 composite exhibited the lowest water absorption, while the F50P50 composite showed the highest. This trend can be attributed to the hydrophilic nature of the jute fibres, which readily absorb moisture due to the presence of hydroxyl groups in their cellulose structure. The composite (F20P80) with a 20% fibre content showed the least water absorption, indicating its lower degree of hydrophilicity, as shown in Fig. 6. A higher proportion of PLA matrix, which is hydrophobic, effectively encapsulates the fibres, reducing the overall water uptake. With an increase to 30% fibre content (F30P70), the water absorption increased. This is due to the higher availability of fibres that can absorb water, although the PLA matrix still provides a significant barrier. At a 40% fibre content (F40P60), the water absorption continued to rise.

This composition balances the fibre and matrix content, leading to a notable increase in water uptake due to the higher fibre presence. The composite with 50% fibre content (F50P50) exhibited the highest water absorption. The high fibre content provides more sites for moisture ingress, and the reduced PLA matrix content is less effective in preventing water uptake. The increase in water absorption with a higher fibre content has important implications for the mechanical performance and durability of the biocomposites. The water absorbed by the fibres can lead to swelling, debonding at the fibre–matrix interface, and degradation of the mechanical properties. Therefore, although a higher fibre content enhances certain mechanical properties, it also necessitates careful consideration of moisture resistance for applications in humid or wet environments.

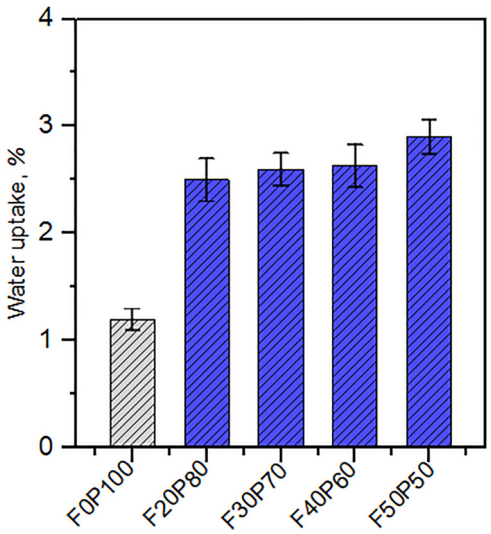

Fig. 6 Water uptake percentage of UD jute-PLA biocomposites with respect to fibre content.

3.4 Microstructural observations

The microstructure of the composites was initially examined using optical microscopy at 250× magnification. This analysis focused on the effect of fiber content on the distribution of jute fibers within the composites (see Fig. 7). At a lower fiber content of 20%, the fibers were more uniformly distributed throughout the composite (Fig. 7a). However, with an increase in the fiber content to 30% and 40%, noticeable fiber agglomeration occurred, likely due to the combined effects of the PVA binder and the compression applied during preforming and composite fabrication (see Fig. 7c and d). Interestingly, as shown in Fig. 7d, a more uniform fiber distribution is observed at a higher fiber loading, which may be attributed to the optimized combination of compression and the maximum fiber content, ultimately resulting in improved fiber dispersion within the composite.

The SEM micrographs of the fracture specimens after the tensile test were examined with respect to different fibre contents (20–40%), as shown in Fig. 8. This study examines the

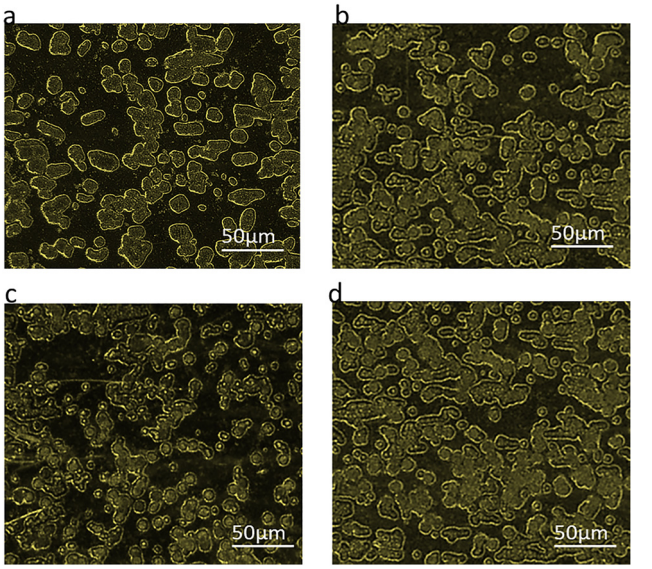

Fig. 7 Optical micrographs of the different composites 250× magnification: (a) composite cross section at 20% fiber content, (b) composite cross section at 30% fiber content, (c) composite cross section at 40% fiber content, and (d) composite cross section at 50% fiber content.

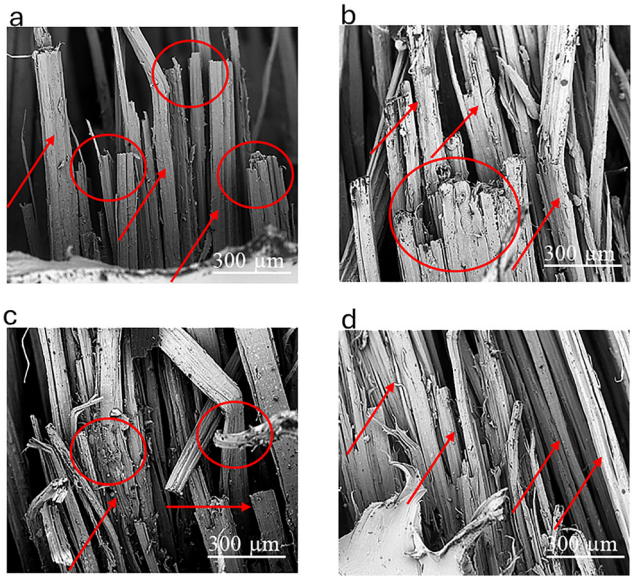

Fig. 8 SEM micrograph of UD jute-PLA biocomposites tensile fractured specimens: (a) fracture specimen of F20P80 composites, (b) fracture specimen of F30P70 composites, (c) fracture specimen of F40P60 composites, and (d) fracture specimen of F50P50 composites.

SEM images of the jute-PLA-based biocomposites with different fibre volume fractions (20%, 30%, 40%, and 50%). The goal is to understand how varying fibre contents influence the fracture behaviour and interfacial bonding in these biocomposites.

Scanning electron microscopy (SEM) analysis of the F20P80 composite revealed a relatively smooth fracture surface with limited evidence of fibre pull-out (see Fig. 8a). The fibres appeared to be uniformly distributed and strongly bonded to the PLA matrix, suggesting their effective interfacial adhesion. At this low fibre loading, the composite exhibited characteristics of ductile failure, with significant matrix deformation and linear fibre fracture. This behavior indicates that a reduced fibre content enhances the ability of the matrix to absorb and dissipate fracture energy, thereby improving the toughness of the material. In contrast, the SEM images of the F30P70 composite (see Fig. 8a and b) displayed a higher incidence of fibre pull-out. Although the fibre distribution remained uniform, visible voids between the fibres and matrix were observed, implying the onset of interfacial debonding. The fracture morphology featured a combination of ductile and brittle failure mechanisms, with evidence of both matrix plastic deformation and fibre fracture. These observations suggest that an increase in fibre content begins to hinder effective stress transfer at the fibre–matrix interface. The SEM images of the F40P60 composite indicate significant fibre pull-out and larger voids between the fibres and the matrix (see Fig. 8c). A higher fibre content results in more pronounced interfacial debonding and some fibre agglomeration. The fracture surface predominantly exhibits brittle failure characteristics. There is a noticeable increase in fibre breakage and pull-out, which points to weaker interfacial bonding. The matrix shows limited plastic deformation, suggesting that the fibres play a more dominant role in the load-bearing process. The SEM images of the F50P50 composite reveal extensive fibre pull-out and large voids between the fibres and the matrix (see Fig. 8d). Poor fibre dispersion and significant agglomeration are evident. The fracture surface is characterized by predominantly brittle failure modes. The poor interfacial bonding and high fibre content result in substantial fibre pull-out and breakage, with minimal matrix deformation. This indicates the reduced ability of the composite to absorb energy during fracture, compromising its mechanical performance.

3.5 Thermal analysis

Thermogravimetric analysis (TGA) and differential thermogravimetric (DTG) analysis have been used to study the thermal stability and decomposition behaviour of the composite materials. This analysis helps in understanding the degradation mechanisms and thermal properties of jute-PLA biocomposites with varying fibre contents (20%, 30%, 40%, and 50%). As shown in Fig. 9a, the TGA curve shows a small mass loss for the composites with a fibre content in the range of 20–40% at around 100 °C, which can be attributed to the evaporation of absorbed moisture. However, this mass loss drastically falls when the fibre content reaches the maximum of 50%, confirming the hydrophilic nature of the jute fibre in thermal environments.

Considering the major decomposition area in the TGA curves of all the composites, it shows clear evidence that up to 50% fibre content in the jute-PLA biocomposites results in major mass loss in the temperature range of 300 °C–400 °C. However, the intensity of mass loss for the F50P0 composite is higher than that of the other composites, confirming its lower thermal stability in this temperature range. The same trend is followed at the pyrolysis temperature of 600 °C.

As shown in Fig. 9b, DTG provides the rate of mass loss as a function of temperature, highlighting the temperature at which the maximum decomposition occurs. In the case of the F20P80 composite, its DTG curve shows a single prominent peak at around 350 °C, corresponding to the maximum decomposition rate of the PLA matrix. In the case of the F30P70 composite, its DTG curve still shows a single peak at around 350 °C, but with a slightly lower peak height, indicating a reduced rate of PLA degradation due to the presence of more fibres. Similar to these composites, the DTG curve of the F40P60 composite exhibits a broader peak at around 350 °C with a further reduced height, suggesting improved thermal stability and a slower decomposition rate with higher fibre content. In contrast, the DTG curve of the F50P50 composite shows a broader and less intense peak, indicating a significantly slower decomposition rate. This is due to the high fibre content of this composite, which enhances its thermal stability.

3.6 Comparative study with the literature

In this study, the tensile properties of the developed composite have been compared with that of other natural fibre PLA-based composites to determine the efficacy of the newly developed UD preform-based composites, as shown in Table 4. A direct

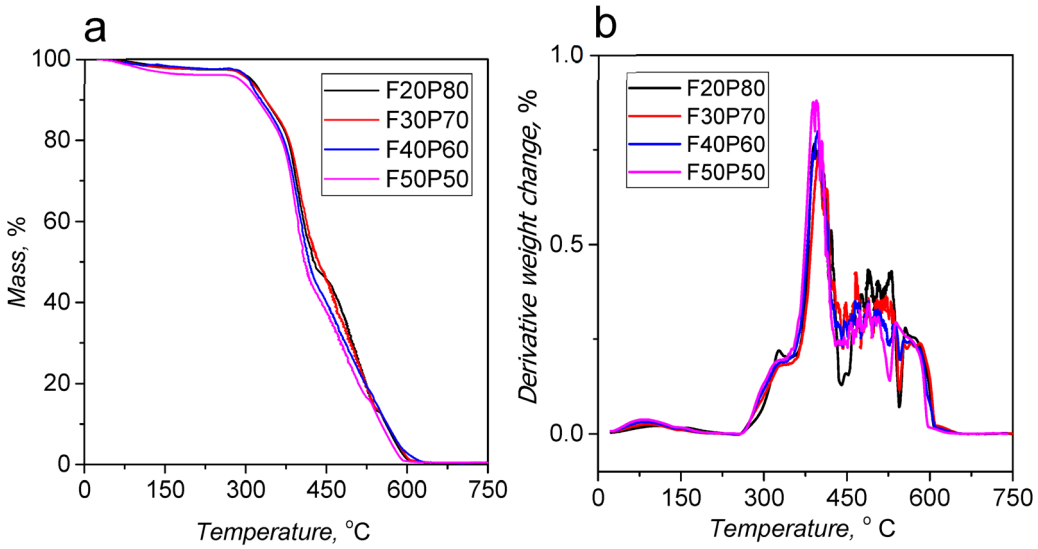

Fig. 9 Thermal analysis of jute/PLA biodegradable composites: (a) TGA analysis and (b) DTG analysis.

Table 4 Comparison of tensile and flexural strengths of different composites

Plant/synthetic fibre-reinforced composites	Fibre type	Tensile strength (MPa)	Tensile modulus (GPa)	Tensile strain (%)	Flexural strength (MPa)	Flexural modulus (GPa)	Ref.
Kenaf/PLA (40 wt%)	—	—	—	—	40	6	55
Kenaf/PLA (40 vol%)	—	60	6.4	2%	—	—	56
Coir/PLA	—	5	1.5	0.7%	25	3.2	57
Coir/PLA	—	8	0.4	3.4%	20	1.4	57
Kenaf/coir/PLA	—	100	7	—	—	—	58
Flax/PLA	Random	83	9.3	—	130	—	59
Flax/PLA	Aligned	151	18.5	—	215	—	59
Flax/PLA	—	99	16		140	—	60
Jute/flax/PLA	—	61.89	17.75	1.9%	—	—	61
Lyocell/PLA (40 wt%)	—	89	9.3	—	—	—	62
Jute/PLA (40%) fabric	Fabric	45	17.8	1.28%	—	—	63
Jute/PLA (34%) short fibre	Short fibre	79	5	—	—	—	64
Jute/PLA	Short fibre	90.7	12.3	—	—	—	65
Jute/PLA (5% NaOH treated)	—	55	1.7	—	110	—	66
Jute/PLA (GO modified)	—	61.71	4.34	—	97.39	7.30	67
Jute/PLA (20%)	UD fibre						This study
Jute/PLA (30%)	UD fibre						This study
Jute/PLA (40%)	UD fibre						This study
Jute/PLA (50%)	UD fibre	187.1	5.13		91.77	5.872	This study

comparison cannot always be considered given that the employed technique, fibre consolidation process, fibre preparation (retting), and measurements of fibre properties are largely variable. The following comparison considered the closest fibre volume content, method of composite manufacturing, *etc.* The following table summarizes the key mechanical properties, highlighting the effectiveness of jute fibres as a reinforcement in PLA-based composites. The tensile strength of the jute/PLA composite in this study is more than double that of kenaf and coir-based PLA composites (60–100 MPa). This shows the superiority of jute fibres in strengthening PLA composites. The flexural strength of 91.77 MPa for the jute/PLA composite is also one of the highest among the listed materials, outperforming similar composites reinforced with kenaf and coir fibres. The modulus of the developed composite is lower than that of a flax/PLA composite but still offers good stiffness, showing that jute is a viable alternative for composite reinforcement. These results suggest that jute fibres can be effectively used to reinforce PLA for applications requiring strong, lightweight, and environmentally friendly materials. Further optimization and testing can enhance the mechanical performance even further.

4. Conclusion

PLA biocomposites were prepared using the compression moulding technique. Field-retted jute fibres were collected and processed into dry fibre preforms through manual hackling to enhance fibre alignment and packing density. The composite

materials were produced using the film-stacking technique, in which PLA films were alternately layered with the jute fibre preforms. The influence of varying fibre content on the mechanical performance, thermal stability, and water absorption behaviour of the composites was systematically investigated. In addition, multiple numerical modelling approaches were employed to support and corroborate the experimental observations. The principal outcomes of this study are as follows:

- The incorporation of a small percentage of compressed jute fibre significantly improved the tensile and flexural properties of the composites compared to neat PLA, suggesting their potential for load-bearing applications.
- Increasing the fibre content consistently enhanced the mechanical properties, supporting the rule of mixtures. An optimal fibre content of approximately 50% yielded the highest performance, with a tensile strength of ~187.1 MPa, tensile modulus of ~5.13 GPa, flexural strength of ~91.77 MPa, and flexural modulus of ~5.82 GPa, confirming their suitability for structural composite applications.
- The tensile strength of the composites was effectively predicted using various numerical models, including the rule of mixtures, Halpin-Tsai equation, Kelly-Tyson model, and Cox model. Nonetheless, notable deviations were identified between the predicted and experimental values for tensile modulus. These inconsistencies are likely attributed to factors such as non-uniform fibre orientation within the preforms, the presence of contaminants, and inconsistent interfacial adhesion between the fibres and the polymer matrix.
- Thermal analysis showed a slight decrease in both onset and final degradation temperatures with an increase in fibre content, although the changes were not substantial. Water absorption increased with higher fibre content, which is attributed to the greater number of –OH functional groups present in natural jute fibres.
- A comparative analysis with the existing literature reveals that this study achieved the highest reported tensile strength for jute/PLA-based biocomposites, indicating a significant advancement in performance.

Overall, the study highlights the potential of field-retted jute fibres in the fabrication of high-performance UD jute/PLA biocomposites, particularly for structural applications.

Conflicts of interest

There are no conflicts to declare.

Data availability

The data that support the findings of this study are available from the corresponding author upon reasonable request.

References

1 F. Sarker, N. Karim, S. Afroj, V. Koncherry, K. S. Novoselov and P. Potluri, High-Performance Graphene-Based Natural Fiber Composites, *ACS Appl. Mater. Interfaces*, 2018, **10**(40), 34502–34512, DOI: **10.1021/acsami.8b13018**.

2 H. Burrola-Núñez, P. J. Herrera-Franco, D. E. Rodríguez-Félix, H. Soto-Valdez and T. J. Madera-Santana, Surface modification and performance of jute fibers as reinforcement on polymer matrix: An overview, *J. Nat. Fibers*, 2019, **16**(7), 944–960.

3 M. A. Rashid, M. A. Islam, M. N. Hasan, M. N. N. Anu and M. H. Ikbal, A critical review of dynamic bonds containing curing agents for epoxy resin: Synthesis, challenges, and emerging applications, *Polym. Degrad. Stab.*, 2024, **229**, 110980, DOI: **10.1016/J.POLYMDEGRADSTAB.2024.110980**.

4 A. Mandal, *et al.*, Integration of recycled denim waste cotton fibre and jute fibre in thermoplastic bio composite applications, *Results Mater.*, 2024, **23**, 100611, DOI: **10.1016/J.RINMA.2024.100611**.

5 M. A. Rashid, J. H. Emon, M. A. Islam and M. N. Hasan, Effect of Methoxy Groups on the Structure-Properties Relationship of Lignin-Derived Recyclable Epoxy Thermosets, *ACS Appl. Polym. Mater.*, 2024, **6**(15), 9312–9322, DOI: **10.1021/ACSAPM.4C01744/SUPPL_FILE/AP4C01744_SI_001.PDF**.

6 S. Kane, E. Van Roijen, C. Ryan and S. Miller, Reducing the environmental impacts of plastics while increasing strength: Biochar fillers in biodegradable, recycled, and fossil-fuel derived plastics, *Compos., Part C: Open Access*, 2022, **8**, 100253, DOI: **10.1016/J.JCOMC.2022.100253**.

7 A. Seile, E. Spurina and M. Sinka, Reducing Global Warming Potential Impact of Bio-Based Composites Based of LCA, *Fibers*, 2022, **10**(9), 79, DOI: **10.3390/FIB10090079/S1**.

8 K. J. Bavaliya, N. S. Vala, M. Raj and L. Raj, A review on biodegradable composites based on poly (lactic acid) with various bio fibers, *Chem. Pap.*, 2024, **78**(5), 2695–2728, DOI: **10.1007/S11696-023-03298-X**.

9 D. B. Dittenber and H. V. S. Gangarao, Critical review of recent publications on use of natural composites in infrastructure, *Composites, Part A*, 2012, **43**(8), 1419–1429, DOI: **10.1016/J.COMPOSITESA.2011.11.019**.

10 P. Lertwattanaruk and A. Suntijitto, Properties of natural fiber cement materials containing coconut coir and oil palm fibers for residential building applications, *Constr. Build. Mater.*, 2015, **94**, 664–669, DOI: **10.1016/J.CONBUILDMAT.2015.07.154**.

11 A. Karuppasamy, R. Kirubakaran, V. Gopalan, R. Munusamy and K. Krishnasamy, Influences of basalt fiber position and addition on the mechanical and viscoelastic behaviors of steel mesh/flax/basalt fiber metal laminates, *Iran. Polym. J.*, 2024, **34**(8), 1167–1179, DOI: **10.1007/S13726-024-01437-Z/METRICS**.

12 S. O. Han, M. Karevan, M. A. Bhuiyan, J. H. Park and K. Kalaitzidou, Effect of exfoliated graphite nanoplatelets on the mechanical and viscoelastic properties of poly(lactic acid) biocomposites reinforced with kenaf fibers, *J. Mater. Sci.*, 2012, **47**(8), 3535–3543, DOI: **10.1007/S10853-011-6199-8/TABLES/2**.

13 S. O. Han, *et al.*, Understanding the Reinforcing Mechanisms in Kenaf Fiber/PLA and Kenaf Fiber/PP Composites: A

Comparative Study, *Int. J. Polym. Sci.*, 2012, **2012**(1), 679252, DOI: 10.1155/2012/679252.

14 M. S. Huda, L. T. Drzal, A. K. Mohanty and M. Misra, Effect of fiber surface-treatments on the properties of laminated biocomposites from poly(lactic acid) (PLA) and kenaf fibers, *Compos. Sci. Technol.*, 2008, **68**(2), 424–432, DOI: 10.1016/J.COMPSCITECH.2007.06.022.

15 Y. Dong, A. Ghataura, H. Takagi, H. J. Haroosh, A. N. Nakagaito and K. T. Lau, Polylactic acid (PLA) biocomposites reinforced with coir fibres: Evaluation of mechanical performance and multifunctional properties, *Composites, Part A*, 2014, **63**, 76–84, DOI: 10.1016/J.COMPOSITESA.2014.04.003.

16 I. P. Lokantara, J. K. Lim and N. P. G. Suardana, Influence of Water Absorption on Mechanical Properties of Coconut Coir Fiber/Poly-Lactic Acid Biocomposites, *Mater. Phys. Mech.*, 2011, **19**(2), 113–125, Accessed: Jul. 30, 2025. [Online]. Available: https://mpm.spbstu.ru/article/2011.19.2.

17 E. Kasi, S. Ramasamy, R. Kirubakaran, R. Munusamy, E. E. Sudalaimani and A. Karuppasamy, Tensile, Dynamic Mechanical, and Vibration Behavior of Layering Sequence Design Effect of Glass Intertwined Natural Kenaf Woven Polymeric Laminates, *J. Nat. Fibers*, 2024, **21**(1), DOI: 10.1080/15440478.2024.2316791.

18 H. S. S. Shekar and M. Ramachandra, Green Composites: A Review, *Mater. Today: Proc.*, 2018, **5**(1), 2518–2526, DOI: 10.1016/J.MATPR.2017.11.034.

19 M. Farzana, *et al.*, Properties and application of jute fiber reinforced polymer-based composites, *GSC Adv. Res. Rev.*, 2022, **11**(1), 084–094, DOI: 10.30574/GSCARR.2022.11.1.0095.

20 A. Habib, *et al.*, Sustainable Jute Fiber Sandwich Composites with Hybridization of Short Fiber and Woven Fabric Structures in Core and Skin Layers, *Macromol. Mater. Eng.*, 2024, **309**(11), 2400138, DOI: 10.1002/MAME.202400138;PAGE:STRING:ARTICLE/CHAPTER.

21 J. H. Emon, M. A. Rashid, M. A. Islam, M. N. Hasan and M. K. Patoary, Review on the Synthesis, Recyclability, Degradability, Self-Healability and Potential Applications of Reversible Imine Bond Containing Biobased Epoxy Thermosets, *Reactions*, 2023, **4**(4), 737–765, DOI: 10.3390/REACTIONS4040043.

22 M. A. Rashid, M. Y. Ali, M. A. Islam and M. A. Kafi, Investigating the structure-performance correlation of amines based recyclable vanillin epoxy thermosets, *Ind. Crops Prod.*, 2025, **224**, 120303, DOI: 10.1016/J.INDCROP.2024.120303.

23 F. Sarker, P. Potluri, S. Afroj, V. Koncherry, K. S. Novoselov and N. Karim, Ultrahigh Performance of Nanoengineered Graphene-Based Natural Jute Fiber Composites, *ACS Appl. Mater. Interfaces*, 2019, **11**(23), 21166–21176.

24 M. Hasan, A. Saifullah, H. N. Dhakal, S. Khandaker and F. Sarker, Improved mechanical performances of unidirectional jute fibre composites developed with new fibre architectures, *RSC Adv.*, 2021, **11**(37), 23010–23022, DOI: 10.1039/D1RA03515K.

25 A. Surendren, A. K. Mohanty, Q. Liu and M. Misra, A review of biodegradable thermoplastic starches, their blends and composites: recent developments and opportunities for single-use plastic packaging alternatives, *Green Chem.*, 2022, **24**(22), 8606–8636, DOI: 10.1039/D2GC02169B.

26 A. Samir, F. H. Ashour, A. A. A. Hakim and M. Bassyouni, Recent advances in biodegradable polymers for sustainable applications, *npj Mater. Degrad.*, 2022, **6**(1), 1–28, DOI: 10.1038/s41529-022-00277-7.

27 S. Jha, B. Akula, H. Enyioma, M. Novak, V. Amin and H. Liang, Biodegradable Biobased Polymers: A Review of the State of the Art, Challenges, and Future Directions, *Polymers*, 2024, **16**(16), 2262, DOI: 10.3390/POLYM16162262.

28 K. Amulya, R. Katakojwala, S. Ramakrishna and S. Venkata Mohan, Low carbon biodegradable polymer matrices for sustainable future, *Compos., Part C: Open Access*, 2021, **4**, 100111, DOI: 10.1016/J.JCOMC.2021.100111.

29 A. Pokharel, K. J. Falua, A. Babaei-Ghazvini and B. Acharya, Biobased Polymer Composites: A Review, *J. Compos. Sci.*, 2022, **6**(9), 255, DOI: 10.3390/JCS6090255.

30 V. Prasad, A. Alliyankal Vijayakumar, T. Jose and S. C. George, A Comprehensive Review of Sustainability in Natural-Fiber-Reinforced Polymers, *Sustainability*, 2024, **16**(3), 1223, DOI: 10.3390/SU16031223.

31 E. H. Tümer and H. Y. Erbil, Extrusion-Based 3D Printing Applications of PLA Composites: A Review, *Coatings*, 2021, **11**(4), 390, DOI: 10.3390/COATINGS11040390.

32 N. D. Bikiaris, *et al.*, Recent Advances in the Investigation of Poly(lactic acid) (PLA) Nanocomposites: Incorporation of Various Nanofillers and their Properties and Applications, *Polymers*, 2023, **15**(5), 1196, DOI: 10.3390/POLYM15051196.

33 M. K. Gupta, Investigations on jute fibre-reinforced polyester composites: Effect of alkali treatment and poly(lactic acid) coating, *J. Ind. Text.*, 2020, **49**(7), 923–942, DOI: 10.1177/1528083718804203/ASSET/DBBE950E-8FC5-4FAB-9345-777A9267B1D1/ASSETS/IMAGES/LARGE/10.1177_1528083718804203-FIG8.JPG.

34 R. B. Yusoff, H. Takagi and A. N. Nakagaito, Tensile and flexural properties of polylactic acid-based hybrid green composites reinforced by kenaf, bamboo and coir fibers, *Ind. Crops Prod.*, 2016, **94**, 562–573, DOI: 10.1016/J.INDCROP.2016.09.017.

35 G. Lebrun, A. Couture and L. Laperrière, Tensile and impregnation behavior of unidirectional hemp/paper/epoxy and flax/paper/epoxy composites, *Compos. Struct.*, 2013, **103**, 151–160, DOI: 10.1016/j.compstruct.2013.04.028.

36 S. Khandaker, *et al.*, From industrial jute fibre spinning wastes to biofibre-reinforced plastics, *Mater. Chem. Phys.*, 2024, **313**, 128586, DOI: 10.1016/j.matchemphys.2023.128586.

37 A. Orue, A. Jauregi, U. Unsuain, J. Labidi, A. Eceiza and A. Arbelaiz, The effect of alkaline and silane treatments on mechanical properties and breakage of sisal fibers and poly(lactic acid)/sisal fiber composites, *Composites, Part A*, 2016, **84**, 186–195, DOI: 10.1016/j.compositesa.2016.01.021.

38 M. W. Tham, *et al.*, Tensile properties prediction of natural fibre composites using rule of mixtures: A review, *J. Reinf. Plast. Compos.*, 2019, **38**(5), 211–248, DOI: 10.1177/0731684418813650.

39 M. M. Shokrieh and H. Moshrefzadeh-Sani, On the constant parameters of Halpin-Tsai equation, *Polymer*, 2016, **106**, 14–20, DOI: 10.1016/J.POLYMER.2016.10.049.

40 S. Garkhail, R. Heijenrath and T. Peijs, Mechanical properties of natural-fibre-mat-reinforced thermoplastics based on flax fibres and polypropylene, *Appl. Compos. Mater.*, 2000, **7**, 351–372, DOI: 10.1023/A:1026590124038.

41 D. Ray, B. K. Sarkar, A. K. Rana and N. R. Bose, Mechanical properties of vinylester resin matrix composites reinforced with alkali-treated jute fibres, *Composites, Part A*, 2001, **32**(1), 119–127, DOI: 10.1016/S1359-835X(00)00101-9.

42 A. Yeasin, A. Faisal, A. Saifullah, N. D. Hom, S. Alimuzzaman and F. Sarker, Fabrication and Mechanical Performance of Non-Crimp Unidirectional Jute-Yarn Preform-Based Composites, *Molecules*, 2021, **26**(21), 6664, DOI: 10.3390/molecules26216664.

43 H. Cox, The elasticity and strength of paper and other fibrous materials, *Br. J. Appl. Phys.*, 1952, **3**, 72–79, DOI: 10.1088/0508-3443/3/3/302.

44 R. B. Yusoff, H. Takagi and A. N. Nakagaito, A comparative study of polylactic acid (PLA)-Based unidirectional green hybrid composites reinforced with natural fibers such as kenaf, bamboo and coir, *Hybrid Adv.*, 2023, **3**, 100073–100083, DOI: 10.1016/j.hybadv.2023.100073.

45 R. B. Yusoff, H. Takagi and A. N. Nakagaito, Tensile and flexural properties of polylactic acid-based hybrid green composites reinforced by kenaf, bamboo and coir fibers, *Ind. Crops Prod.*, 2016, **94**, 94562–94573, DOI: 10.1016/j.indcrop.2016.09.017.

46 J. I. P. Singh, S. Singh and V. Dhawan, Influence of fiber volume fraction and curing temperature on mechanical properties of jute/PLA green composites, *Polym. Polym. Compos.*, 2020, **28**(4), 273–284, DOI: 10.1177/0967391119872875.

47 M. G. Aruan Efendy and K. L. Pickering, Comparison of strength and Young modulus of aligned discontinuous fibre PLA composites obtained experimentally and from theoretical prediction models, *Compos. Struct.*, 2019, **208**, 566–573, DOI: 10.1016/j.compstruct.2018.10.057.

48 S. Garkhail, R. Heijenrath and T. Peijs, Mechanical properties of natural-fibre-mat-reinforced thermoplastics based on flax fibres and polypropylene, *Appl. Compos. Mater.*, 2000, Accessed: Apr. 28, 2016. [Online]. Available: https://link.springer.com/article/10.1023/A:1026590124038.

49 N. Sultana, *et al.*, Short Jute Fiber Preform Reinforced Polypropylene Thermoplastic Composite: Experimental Investigation and Its Theoretical Stiffness Prediction, *ACS Omega*, 2023, **27**, 24311–24322, DOI: 10.1021/acsomega.3c01533.

50 A. K. Bledzki and J. Gassan, *Composites reinforced with cellulose based fibres*, 1999, DOI: 10.1016/S0079-6700(98)00018-5.

51 I. Taha, A. El-Sabbagh and G. Ziegmann, Modelling of strength and stiffness behaviour of natural fibre reinforced polypropylene composites, *Polym. Polym. Compos.*, 2008, **16**(5), 295–302, DOI: 10.1177/096739110801600502.

52 Y. Du, *et al.*, Kenaf bast fiber bundle-reinforced unsaturated polyester composites. III: Statistical strength characteristics and cost-performance analyses, *Forest Prod. J.*, 2010, **60**(6), 514–521, DOI: 10.13073/0015-7473-60.6.514.

53 J. L. Thomason and M. A. Vlug, Influence of fibre length and concentration on the properties of glass fibre-reinforced polypropylene: 4. Impact properties, *Composites, Part A*, 1997, **28**(3), 277–288, DOI: 10.1016/S1359-835X(96)00127-3.

54 S. Y. Fu and B. Lauke, Effects of fiber length and fiber orientation distributions on the tensile strength of short-fiber-reinforced polymers, *Compos. Sci. Technol.*, 1996, **56**(10), 1179–1190, DOI: 10.1016/S0266-3538(96)00072-3.

55 M. S. Huda, L. T. Drzal, A. K. Mohanty and M. Misra, Effect of fiber surface-treatments on the properties of laminated biocomposites from poly(lactic acid) (PLA) and kenaf fibers, *Compos. Sci. Technol.*, 2008, **68**(2), 424–432, DOI: 10.1016/J.COMPSCITECH.2007.06.022.

56 H. M. Akil, M. F. Omar, A. A. M. Mazuki, S. Safiee, Z. A. M. Ishak and A. Abu Bakar, Kenaf fiber reinforced composites: A review, *Mater. Des.*, 2011, **32**(8–9), 4107–4121, DOI: 10.1016/J.MATDES.2011.04.008.

57 Y. Dong, A. Ghataura, H. Takagi, H. J. Haroosh, A. N. Nakagaito and K. T. Lau, Polylactic acid (PLA) biocomposites reinforced with coir fibres: Evaluation of mechanical performance and multifunctional properties, *Composites, Part A*, 2014, **63**, 76–84, DOI: 10.1016/J.COMPOSITESA.2014.04.003.

58 R. B. Yusoff, H. Takagi and A. N. Nakagaito, Tensile and flexural properties of polylactic acid-based hybrid green composites reinforced by kenaf, bamboo and coir fibers, *Ind. Crops Prod.*, 2016, **94**, 562–573, DOI: 10.1016/J.INDCROP.2016.09.017.

59 M. Akonda, S. Alimuzzaman, D. U. Shah and A. N. M. M. Rahman, Physico-Mechanical, Thermal and Biodegradation Performance of Random Flax/Polylactic Acid and Unidirectional Flax/Polylactic Acid Biocomposites, *Fibers*, 2018, **6**(4), 98, DOI: 10.3390/FIB6040098.

60 P. Georgiopoulos, A. Christopoulos, S. Koutsoumpis and E. Kontou, The effect of surface treatment on the performance of flax/biodegradable composites, *Composites, Part B*, 2016, **106**, 88–98, DOI: 10.1016/J.COMPOSITESB.2016.09.027.

61 M. Ejaz, M. M. Azad, A. U. R. Shah, S. K. Afaq and J. il Song, Mechanical and Biodegradable Properties of Jute/Flax Reinforced PLA Composites, *Fibers Polym.*, 2020, **21**(11), 2635–2641, DOI: 10.1007/S12221-020-1370-Y.

62 N. Graupner and J. Müssig, A comparison of the mechanical characteristics of kenaf and lyocell fibre reinforced poly(lactic acid) (PLA) and poly(3-hydroxybutyrate) (PHB) composites, *Composites, Part A*, 2011, **42**(12), 2010–2019, DOI: 10.1016/J.COMPOSITESA.2011.09.007.

63 M. Ejaz, M. M. Azad, A. U. R. Shah, S. K. Afaq and J. il Song, Mechanical and Biodegradable Properties of Jute/Flax Reinforced PLA Composites, *Fibers Polym.*, 2020, **21**(11), 2635–2541, DOI: 10.1007/s12221-020-1370-y.

64 M. T. Zafar, S. N. Maiti and A. K. Ghosh, Effect of surface treatments of jute fibers on the microstructural and

mechanical responses of poly(lactic acid)/jute fiber biocomposites, *RSC Adv.*, 2016, **6**(77), 73373–73382, DOI: **10.1039/C6RA17894D**.

65 R. Gunti, A. V. Ratna Prasad and A. V. S. S. K. S. Gupta, Preparation and properties of successive alkali treated completely biodegradable short jute fiber reinforced PLA composites, *Polym. Compos.*, 2016, **37**(7), 2160–2170, DOI: **10.1002/PC.23395;PAGEGROUP:STRING:PUBLICATION**.

66 G. Rajesh and A. V. R. Prasad, Tensile Properties of Successive Alkali Treated Short Jute Fiber Reinforced PLA Composites, *Procedia Mater. Sci.*, 2014, **5**, 2188–2196, DOI: **10.1016/J.MSPRO.2014.07.425**.

67 T. Yu, C. Hu and Y. Li, Functionalization of Graphene and Its Influence on Mechanical Properties and Flame Retardancy of Jute/Poly(lactic acid) Composite, *J. Nanosci. Nanotechnol.*, 2019, **19**(11), 7074–7082, DOI: **10.1166/JNN.2019.16659**.